Lithuanian Journal of Physics, Vol. **45**, No. 6, pp. 463–469 (2005)

NUMERICAL MODELLING OF THE ELECTRIC FIELD IN THE SEMICONDUCTOR OBSTACLE PLACED IN THE COAXIAL LINE

Ž. Kancleris, V. Tamošiūnas, and M. Tamošiūnienė

Semiconductor Physics Institute, A. Goštauto 11, LT-01108 Vilnius, Lithuania
E-mail: kancleris@pfi.lt

Received 7 July 2005

In this paper, we present FDTD (finite-difference time-domain) simulation results of the averaged electric field in the semiconductor obstacle placed in the coaxial line. Such layout might be used as a sensing element for the measurement of microwave pulsed power transmitted through the coaxial line. Calculations have been performed for 50 Ω impedance coaxial line filled with air and obstacle made of Si. The dependences of averaged electric field in the obstacle on the microwave frequency, as well as on the height of the obstacle are considered. Situations when the obstacle is placed either on the inner or on the outer conductor of the coaxial line have been investigated.

Keywords: obstacle in the coaxial line, sensor, FDTD method

PACS: 41.20.-q, 07.50.Hp

1. Introduction

The metallic waveguides partially filled with various materials are widely used in constructions of sensors, phase transformers, filters, delay lines, and other equipment for the microwave range. Waveguide type resistive sensor (RS) is a typical example of such devices [1]. It consists of a piece of semiconductor that is placed in the waveguide between a thin metal foil and a wide wall of the waveguide. Resistance of the RS increases due to electron heating in the electric field of a microwave pulse, and the microwave pulse power in the waveguides is determined by measuring this resistance change. Main parameters of the RS such as the sensitivity and reflection coefficient depend on the interaction of the sensing element with electromagnetic wave propagating in the waveguide. Therefore, a detailed study of the guiding devices with the obstacles in them by solving Maxwell equations is a problem of high priority, providing a tool of design of the devices with desirable characteristics.

Different numerical methods have been used to solve the problem of obstacle in the transmission line. A rigorous theory exists [2] for a perfectly symmetrical layout, when symmetrical obstacle replaces a part of coaxial line. However, only several possibilities were explored for non-symmetrical case. For instance, the boundary problem for Maxwell equations has been solved in [3] using the singular integral equations method to calculate the electrodynamic characteristics of the waveguide structure with a low specific resistance semiconductor plate on a narrow partition parallel to the upper wide wall. A singular integral method to solve Maxwell equations that enables one to investigate the waveguide structure containing a semiconductor triangular prism is presented in [4], while a transmission line matrix (TLM) algorithm for cylindrical coordinates was applied in [5] for the frequency-domain investigation of the coaxial line with a sample located near the outer conductor.

In recent years, the finite-difference time-domain (FDTD) [6, 7] method has become one of the most popular methods for the analysis of microwave circuits due to its simplicity and generality in treating complex shapes and material properties. Within FDTD, electromagnetic fields are computed in a discretized space-time domain. The location of the **E** and **H** components in the Yee grid [6] and the central-difference operations on these components implicitly enforce the two Gauss Law relations. Thus, the Yee mesh is divergence-free with respect to its electric and magnetic fields, and thereby properly enforces the absence of free electric and magnetic charge in the source-free space being modelled [7].

However, FDTD is a computer extensive algorithm. This was one of the main reasons why it did not cause

ISSN 1648-8504

great excitement when it was introduced in 1966. The method did not become popular until the early 1980's when computer development and numerical improvements paved the way for FDTD. This method is now widely used in various applications for calculation of waveguide structures consisting of the metallic waveguides with discontinuities in them. Several versions of FDTD have recently been proposed in [8] and [9] to compute the propagation characteristics of cylindrical transmission lines. An absorbing boundary condition was used to truncate the mesh at its outer radial boundary. Several representative cylindrical structures have been investigated.

In this paper, the results of the theoretical FDTD investigation of the averaged electric field in the semiconductor obstacles placed in the coaxial line have been presented. We have investigated the both situations – when the obstacle is placed on the inner and on the outer conductor of the coaxial line. The calculations of the dependences of averaged electric field in the obstacle on the microwave frequency as well as on its height have been performed. The prime objective of our investigations is to find conditions at which the obstacle does not perturb much the coaxial line and the averaged electric field in it is independent on frequency. Such obstacle should serve as a prototype of the coaxial-type RS (CRS). The CRS should keep up the main advantages of the waveguide-type RS (direct measurement of HPM pulse, high output signal) [1] while improving the other main characteristics ("flatness" of frequency response and voltage standing wave ratio (VSWR)).

2. Theoretical consideration of the version of SE

The cross-sectional view of the coaxial line with semiconductor obstacle under consideration is shown in Fig. 1. The height of the obstacle in r direction is indicated as h, the width of the obstacle in φ direction is measured at a middle of the height and is indicated as d, and the length of the obstacle in z direction that is not shown in the plane figure is denoted as l.

Calculations have been performed for the 50 Ω impedance coaxial line filled with air, $\varepsilon_{\rm c} = 1$, and an obstacle made of Si with a relative dielectric constant $\varepsilon = 11.9$. The inner and outer radii of the coaxial line conductors were $r_{\rm i} = 2$ mm, $r_{\rm o} = 4.6$ mm. The modelled section of the coaxial line with the semiconductor obstacle is shown in Fig. 2. The regular wave propagating in the coaxial line is excited in the plane $z = z_{\rm ex}$ by adding oscillating electric field to the computed electric field value. As a result of this

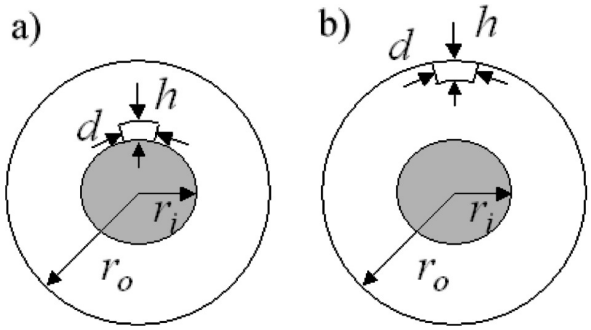

Fig. 1. Cross-sectional view of coaxial line with semiconductor obstacle mounted on (a) inner and (b) outer conductors of the coaxial line. The width d of the obstacle is measured at a middle of the height h; $r_{\rm o}$ and $r_{\rm i}$ are the outer and the inner radii of the conductors of the coaxial line.

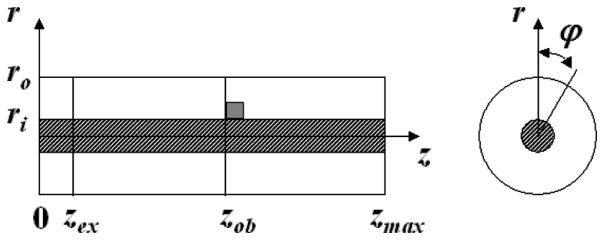

Fig. 2. Model of the coaxial line with semiconductor obstacle used for calculations.

operation, two waves propagating into both sides from the excitation plane are obtained, while the frequency of these waves matches the one of added field. The semiconductor obstacle is placed at a distance approximately corresponding to the wavelength of electromagnetic wave in the coaxial line. Absorbing boundary conditions are satisfied at both ends of the modelled structure. Therefore, the wave propagating left from the excitation plane, as well as the wave reflected from the obstacle, are absorbed in the plane $z = 0$, whereas the wave passed through the obstacle is absorbed into the plane $z = z_{\rm max}$. Components of the electromagnetic field in every point of the line are computed using the FDTD algorithm and these values are used to determine the averaged electric field in the semiconductor obstacle, as well as the reflection coefficient from it.

It is assumed that the electric field components E_φ and E_r should be zero on the surface that limits the obstacle in r direction, when the height of the obstacle is less than the span between conductors. In this way the upper metal contact is accounted in the calculations.

Although the excited wave in the coaxial line has only E_r and H_φ components, all components of electromagnetic field can be excited in the vicinity of the semiconductor obstacle. Therefore, full Maxwell equations have to be solved and all components of electromagnetic field have to be computed in order to

determine the truthful value of electric field in the obstacle. Introducing dimensionless coordinates r/r_0, z/r_0, and time $t \cdot v/r_0$ (where v is a speed of electromagnetic wave in the coaxial line), and measuring magnetic field in electric field units$Z_B H$ (where Z_B is the impedance of free space filled with the same material as the coaxial line), Maxwell equations can be written down in the following way:

$$\frac{\partial \mathbf{E}}{\partial t} = (\nabla \times \mathbf{H} - \gamma \mathbf{E}) \frac{\varepsilon_c}{\varepsilon}\,, \tag{1}$$

$$\frac{\partial \mathbf{H}}{\partial t} = -\nabla \times \mathbf{E}\,. \tag{2}$$

Here $\gamma = Z_B r_0/\rho$, where ρ is the specific resistance of the semiconductor obstacle. In (2) it is assumed that the relative magnetic constant of the coaxial line and semiconductor obstacle is equal 1. By taking this into account, the speed of electromagnetic wave in the coaxial line and the impedance of free space can be easily found from these expressions:

$$v = \frac{1}{\sqrt{\varepsilon_c \varepsilon_0 \mu_0}}\,, \tag{3}$$

$$Z_B = \frac{\mu_0}{\sqrt{\varepsilon_c \varepsilon_0}}\,, \tag{4}$$

where ε_0, μ_0 are permittivity and permeability of free space, respectively. Propagation of the wave outside the obstacle is also described by equations (1) and (2) with $\gamma = 0$ and $\varepsilon = \varepsilon_c$.

Equations (1) and (2) can be solved numerically using FDTD method. To this aim, at the first step they should be written down explicitly in cylindrical coordinates, leading to six equations, which relate three components of vector $\mathbf{E}(E_r, E_\varphi, E_z)$ and three components of vector $\mathbf{H}(H_r, H_\varphi, H_z)$. The mesh points where the components of electromagnetic field are calculated are shifted by a half of step [6–9]. The elementary cell of the conventional 3D FDTD lattice in cylindrical coordinates can be chosen in the way shown in Fig. 3. It is seen that there are four points located on the middle of the each edge in the elementary cell, where electric field components are calculated, whereas magnetic field components are computed in the two points that are located in the middle of the surfaces that comprise the elementary cell. Choosing elementary cell in such a way, the boundary conditions at any direction should be satisfied by corresponding electric field components. Meanwhile the magnetic field component lying on the boundary surface is calculated by making use of four electric field component values already determined from the boundary condition. It should be mentioned that electric and magnetic field components are determined at different time moments, therefore

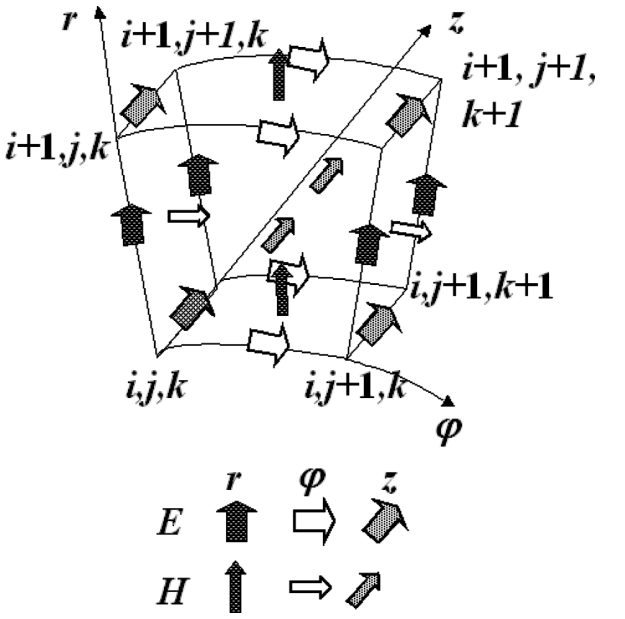

Fig. 3. Elementary 3D FDTD cell in cylindrical coordinates. The arrows denote the points where particular component of electromagnetic field is calculated. A legend of the components of electromagnetic field is shown in the lower part of the figure.

$$H_r \Rightarrow H^{(n+1/2)}_{r_{(i,j+1/2,k+1/2)}}\,, \quad E_r \Rightarrow E^{(n)}_{r_{(i+1/2,j,k)}}\,,$$

$$H_\varphi \Rightarrow H^{(n+1/2)}_{\varphi_{(i+1/2,j,k+1/2)}}\,, \quad E_\varphi \Rightarrow E^{(n)}_{\varphi_{(i,j+1/2,k)}}\,, \tag{5}$$

$$H_z \Rightarrow H^{(n+1/2)}_{z_{(i+1/2,j+1/2,k)}}\,, \quad E_z \Rightarrow E^{(n)}_{z_{(i,j,k+1/2)}}\,.$$

The upper index corresponds to the number of the time step, while the lower – to the number of the coordinate step in these expressions: $i \Rightarrow r$, $j \Rightarrow \varphi$, and $k \Rightarrow z$. In the first time step the new values of magnetic field components are evaluated using previous values of components calculated earlier, while in the next step the values of magnetic field components are used to update electric field component values. As it was already mentioned, outside the semiconductor obstacle $\gamma = 0$ and $\varepsilon = \varepsilon_c$.

Electric and magnetic field components can be calculated at any point of the modelled structure at any time moment. A regular varying in time electric field component E_r is added to the calculated value in the plane $z = z_{\rm ex}$ providing two regular waves propagating to the right and left sides from the excitation plane. Therefore, frequency of E_r variation defines the frequency of the waves inside the entire simulation domain. To get a stationary solution of the problem the initial and boundary conditions have to be formulated.

At $t = 0$ there is no any electric or magnetic field in the coaxial line, therefore all components of electric and magnetic field should be zero. When the dimensions of the semiconductor obstacle are much less than the characteristic dimensions of the coaxial line, the stationary solution is obtained faster when the initial regular wave is inserted into modelled structure.

As it was already mentioned, the boundary conditions should be formulated for the corresponding components of the electric field only when using elementary 3D FDTD cell shown in Fig. 3. As can be easily seen from the figure, the components E_φ and E_r should satisfy non-reflecting boundary conditions in the planes $z = 0$ and $z = z_{\max}$. Electric field components lying in the conductor surfaces should be zero on the inner and outer conductors:

$$E_\varphi(r_\mathrm{i}, \varphi, z) = 0\,, \quad E_\varphi(r_\mathrm{o}, \varphi, z) = 0\,,$$

$$E_z(r_\mathrm{i}, \varphi, z) = 0\,, \quad E_z(r_\mathrm{o}, \varphi, z) = 0\,. \tag{6}$$

Using considered initial and boundary conditions a stationary solution is obtained by modelling a few periods of oscillations. After each period, the amplitudes of electric field component E_r in the plane crossing the centre of the obstacle have been determined. The obtained amplitudes are compared with the corresponding values calculated one period before. If the difference between them is less than predefined value δ, the calculations are stopped and amplitudes of electromagnetic field components calculated during the last period are considered as a stationary solution. Otherwise, next successive period of oscillations is modelled. To achieve 3% accuracy for moderate size obstacle 3–4 periods of oscillations should be modelled.

It should be noted that due to the linearity of Maxwell equations the solution could be scaled to the other dimensions of the coaxial line by a corresponding change of dimensions of the obstacle, its specific resistance, and the frequency of the microwave. For example, let's assume that the calculation has been performed for the coaxial line with inner and outer radii r_i, r_o and for the obstacle with dimensions h, d, l and specific resistance ρ at microwave wavelength λ. Distribution of electromagnetic field components will be the same in the obstacle placed in the coaxial line of other dimensions r'_i, and r'_o with recalculated values of the parameters h', d', l', ρ', and λ' using simple transformation formula

$$p' = \frac{p}{r_\mathrm{o}} r'_\mathrm{o}\,, \tag{7}$$

here p and p' represent h, d, l, ρ, λ and h', d', l', ρ', λ', respectively.

It is worth to mention that calculated amplitudes of electric and magnetic field components were normalized to the electric field strength on the inner conductor of the empty coaxial line. Therefore when the absolute values of those amplitudes are determined for the coaxial line with other dimensions, the normalization constant should be recalculated according to the expression

$$E_\mathrm{norm} = 84.796 \sqrt{\frac{P}{\varepsilon Z_\mathrm{C}}} \frac{1}{r'_\mathrm{i}}\,, \tag{8}$$

where P is a pulse power and Z_C is an impedance of the coaxial line.

The example of the solution scaling is shown in Table 1. As one can see, the identical solution for a larger coaxial line is obtained for the obstacle, when the dimensions and specific resistance of it are increased proportionally to the dimensions of the coaxial line. It is obvious that the same solution is obtained at lower frequency for a larger coaxial line. The electric field strength on the inner surface of the conductor decreases as well.

It is of interest to compare the calculated values of averaged electric field in the obstacle with the values in the ideal obstacle that does not perturb the distribution of electromagnetic field components in the empty coaxial line. Average electric field in the ideal obstacle being placed on the inner conductor can be expressed as follows:

$$\frac{\langle E_r \rangle}{E_r(r_\mathrm{i})} = \frac{r_\mathrm{i}}{h} \int\limits_{r_\mathrm{i}}^{r_\mathrm{i}+h} \frac{\mathrm{d}r}{r} = \frac{r_\mathrm{i}}{h} \ln\left(\frac{r_\mathrm{i}+h}{r_\mathrm{i}}\right). \tag{9}$$

Analogous formula describes average electric field in the ideal obstacle placed on the outer conductor of the coaxial line:

$$\frac{\langle E_r \rangle}{E_r(r_\mathrm{i})} = \frac{r_\mathrm{i}}{h} \int\limits_{r_\mathrm{o}-h}^{r_\mathrm{o}} \frac{\mathrm{d}r}{r} = \frac{r_\mathrm{i}}{h} \ln\left(\frac{r_\mathrm{o}}{r_\mathrm{o}-h}\right). \tag{10}$$

3. Results and discussion

We perform calculation for an obstacle of sufficiently small cross-sectional size, namely, $l = d = 1.5$ mm. These dimensions have been selected since our task is to find the obstacle that is not perturbing much the coaxial line. Calculation results of the averaged electric field component E_r for the obstacle placed on the inner and outer conductors with specific resistance $\rho = 30\ \Omega{\cdot}$cm having different height h are

Table 1. Parameters of the obstacles that correspond to the same solution of Maxwell equations for different size of the coaxial line.

Coax. type	r_o, mm	r_i, mm	ρ, Ω·cm	h, mm	l, mm	V/cm at P=1 kW	λ, cm	f, GHz
5/2	4.605	2.00	5.00	1.00	1.50	1896	3.00	10.00
7/3	6.906	3.00	7.50	1.50	2.25	1264	4.50	6.67
8/3.5	8.086	3.50	8.78	1.76	2.63	1083	5.26	5.70

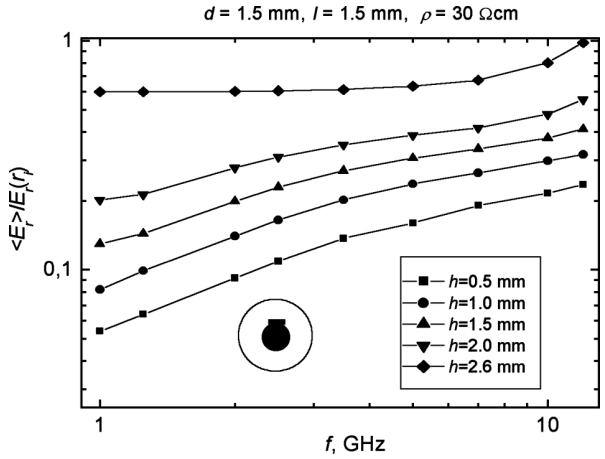

Fig. 4. Dependences of the averaged amplitude of the electric field component E_r in the semiconductor obstacle placed on the inner conductor on the microwave frequency for different height of the obstacle. Electric field strength is normalized to its value on the inner conductor of an empty coaxial line. $r_o = 4.605$ mm, $r_i = 2.0$ mm, $\varepsilon_c = 1$, $d = 1.5$ mm, $l = 1.5$ mm, $\varepsilon = 11.9$, $\rho = 30$ Ω·cm. The height is indicated on figure. At $h = 2.6$ mm the obstacle covers the span between conductors.

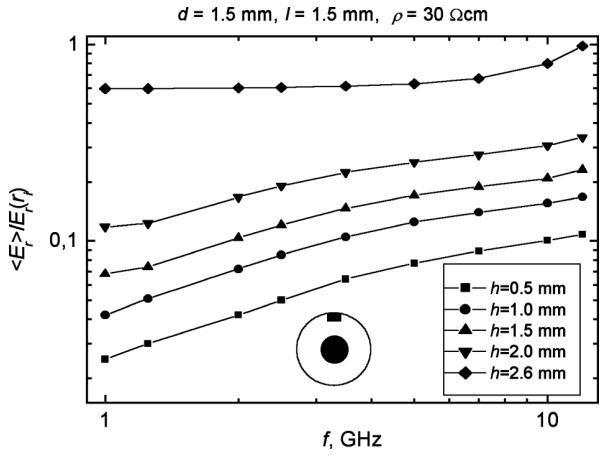

Fig. 5. Dependences of the averaged amplitude of the electric field component E_r in the semiconductor obstacle placed on the outer conductor on the microwave frequency for different height of the obstacle. Electric field strength is normalized to its value on the inner conductor of an empty coaxial line. $r_o = 4.605$ mm, $r_i = 2.0$ mm, $\varepsilon_c = 1$, $d = 1.5$ mm, $l = 1.5$ mm, $\varepsilon = 11.9$, $\rho = 30$ Ω·cm. The height is indicated on figure. At $h = 2.6$ mm the obstacle covers the span between conductors.

shown in Figs. 4 and 5. As one can see from the figures, calculated dependences of $\langle E_r \rangle$ on frequency qualitatively are identical for the different height obstacles placed either on inner or on outer conductors of the coaxial line. The values of averaged electric field in the obstacles placed on the inner and the outer conductors differ roughly by two times that approximately corresponds to the ratio of electric field strength on the inner and outer conductors in an empty 50 Ω impedance coaxial line ($E_r(r_i)/E_r(r_o) = 2.3$).

When the height of the obstacle increases, the averaged electric field in it grows up as well. $\langle E_r \rangle$ becomes nearly independent on frequency in low frequency region when the obstacle covers the gap between the conductors of the coaxial line, while the averaged electric field strength increases in high frequency limit. The field distribution analysis reveals that this effect should be attributed to the resonant excitation of transverse electric mode TE_{11} in a region near the sample.

The rudiments of the TE_{11} mode also appear in the coaxial line in the case when the height of obstacle is smaller than the span between inner and outer conductors. TE_{11} mode is excited in the neighbourhood of the obstacle and does not propagate further due to a mismatch of the effective dielectric constant.

Table 2. Electric field strength in the ideal obstacle that does not perturb the distribution of electric field in the empty coaxial line (calculated from expressions (9) and (10)).

	inner		outer	
	h=0.5 mm	h=1.0 mm	h=0.5 mm	h=1.0 mm
$\frac{\langle E_r \rangle}{E_r(r_i)}$	0.893	0.811	0.461	0.509

It is worth to mention that the averaged electric field value is roughly 0.6 in a low frequency limit and this value is very close to the one calculated for an ideal obstacle (0.64) using expressions (9) or (10) (presented in Table 2).

Careful inspection of the curves presented in Figs. 4 and 5 reveal that the turning point in the dependences $\langle E_r \rangle(f)$ can be distinguished for $\rho = 30$ Ω·cm at $f_c = 5$ GHz. It is clearly seen that below this frequency the decrease of $\langle E_r \rangle$ with decreasing f is more pronounced in comparison with the frequency range $f > f_c$.

It might be pointed out that when the height of the obstacle is less than the span between inner and outer conductors the obstacle placed either on inner or on outer conductors might be treated as semi insulating capacitor. This "capacitor" can be charged to higher potential when the displacement current prevails over conductivity one. Therefore, averaged electric field inside the obstacle is larger and the dependence of averaged electric field strength on frequency should be less pronounced. At lower frequencies conductivity current prevails over the displacement current and blocks the charging of the capacitance. Because of this reason the averaged electric field in the obstacle decreases more rapidly at lower frequencies. The frequency at which conductivity current becomes equal to the displacement one can be easily calculated by comparing the amplitudes of the displacement and conductivity currents at the same electric field amplitude. The threshold point for the frequency can be determined using expression

$$f_{\mathrm{c}} = \frac{1}{2\pi\varepsilon\varepsilon_0\rho}\,. \tag{11}$$

Inserting into (11) the values of ρ and ε one can get that $f_{\mathrm{c}} = 5.3$ GHz that is close to the threshold point determined from our calculations.

Calculated reflection coefficient for 0.5 and 1 mm height obstacles was sufficiently small. VSWR is less than 1.15 at 12 GHz and decreases down to 1.01 at 1 GHz for the obstacle placed on the inner conductor. VSWR is even lower: 1.04 at 12 GHz and 1.005 at 1 GHz for the obstacle placed on the outer conductor.

4. Conclusions

It was obtained that the averaged electric field in the obstacle that does not cover the gap between the conductors of the coaxial line is frequency dependent. The decrease of the averaged electric field $\langle E_r \rangle$ with decreasing frequency f is more pronounced for frequencies below $f_{\mathrm{c}} = 5$ GHz in comparison with the frequency range $f > f_{\mathrm{c}}$ when $\rho = 30\ \Omega{\cdot}$cm.

When the obstacle covers the gap between the conductors of the coaxial line, the averaged electric field strength $\langle E_r \rangle$ in the obstacle is independent of frequency in low frequency region, while it increases in high frequency limit. It was cleared up that the excitation of TE_{11} mode in the coaxial line in the neighbourhood of the obstacle is responsible for this increase. For this type obstacle the value of the averaged electric field is roughly 0.6 in a low frequency limit and this value is very close to the one calculated for an ideal obstacle (0.64). It seems that this type of obstacle is more suitable for the CRS design.

Acknowledgement

This work was partly supported by the Lithuanian State Science and Studies Foundation through the program "Advanced Millimetre-Wave Electronics".

References

[1] M. Dagys, Ž. Kancleris, R. Simniškis, E. Schamiloglu, and F.J. Agee, Resistive sensor: Device for high-power microwave pulse measurement, IEEE Antennas Propag. Mag. **43**(5), 64–79 (2001).

[2] R. Beliackas, J. Grigas, A. Orliukas, and V. Shugurov, Dielectric dispersion in SbSJ crystals, Lithuanian J. Phys. **11**(6), 1029–1038 (1971).

[3] V. Tamošiūnas, V. Shugurov, M. Tamošiūnienė, K.F. Berggren, and L. Knishevskaya, Computation of electric field components and standing wave coefficient for a wavequide structure with a lowohm semiconductor plate, Int. J. Infrared Millimeter Waves **21**(11), 1831–1835 (2000).

[4] V. Tamošiūnas, V. Shugurov, M. Tamošiūnienė, K.F. Berggren, and L. Knishevskaya, Computation of the reflection coefficient of a triangular semiconductor prism in a rectangular waveguide, Int. J. of Infrared and Millimeter Waves **21**(7), 1113–1117 (2000).

[5] J. Huang, K. Wu, P. Morin, and C. Akyel, Characterization of highly dispersive materials using composite coaxial cells: Electromagnetic analysis and wideband measurements, IEEE Trans. Microwave Theory Tech. **44**(5), 770–777 (1996).

[6] K.S. Yee, Numerical solution of initial boundary problems involving Maxwell's equation in isotropic media, IEEE Trans. Antennas Propag. **14**(3), 302–307 (1966).

[7] A. Taflove, *Computational Electrodynamics. The Finite-Difference Time-Domain Method* (Artech House, Norwood MA, 1995).

[8] N. Dib, T. Weller, M. Scardelletti, and M. Imparato, Analysis of cylindrical transmission lines with the finite-difference time-domain method, IEEE Trans. Microwave Theory Tech. **47**(4), 509–512 (1999).

[9] Y. Chen, R. Mitra, and P. Harms, Finite different time domain algorithm for solving Maxwell's equation in rotationally symmetric geometries, IEEE Trans. Microwave Theory Tech. **44**(6), 832–838 (1996).

ELEKTRINIO LAUKO PUSLAIDININKINĖJE KLIŪTYJE, KURI YRA BENDRAAŠĖJE LINIJOJE, SKAITMENINIS MODELIAVIMAS

Ž. Kancleris, V. Tamošiūnas, and M. Tamošiūnienė

Puslaidininkių fizikos institutas, Vilnius, Lietuva

Santrauka

Baigtinių skirtumų laiko skalėje metodu (FDTD) ištirtos elektrinio lauko puslaidininkinėje (Si) kliūtyje, esančioje bendraašėje linijoje, priklausomybės nuo dažnio f skirtingo aukščio h kliūtims. Ištirti du atvejai: (i) kliūtis patalpinta ant vidinio laidininko paviršiaus, (ii) kliūtis – ant išorinio laidininko. Tirta bendraašė linija tarp išorinio ir vidinio laidininkų užpildyta oru, jos banginė varža buvo lygi 50 Ω. Bendraašės linijos vidinio laidininko spindulys $r_{\rm i} = 2$ mm, o išorinio – $r_{\rm o} = 4,6$ mm. Kliūties aukštis h buvo matuojamas linijos spindulio kryptimi. Silicio, iš kurio pagaminta kliūtis, santykinė dielektrinė skvarba $\varepsilon = 11,9$. Nors bendraaše linija sklinda reguliari banga, turinti tik E_r ir H_φ dedamąsias, kliūties aplinkoje susižadina visos elektromagnetinio lauko dedamosios, kurios ir buvo skaičiuojamos visoje modeliuojamoje bendraašės linijos atkarpoje su kliūtimi.

Apskaičiuotos elektrinio lauko stiprio vertės buvo normuotos į elektrinio lauko stiprio vertę ant vidinio laidininko paviršiaus tuščioje bendraašėje linijoje. Elektrinio lauko stiprio priklausomybės nuo dažnio f (f vertės kito nuo 1 iki 12 GHz) apskaičiuotos, kai kliūties aukščio h vertės kito nuo 0,5 iki 2,6 mm. Kai kliūties, kurios savitoji varža $\rho = 30$ Ω·cm, aukštis padidėja, vidutinė elektrinio stiprio vertė taip pat padidėja. Kai $h = 2,6$ mm, kliūtis užpildo visą tarpą tarp vidinio ir išorinio laidininkų (spindulio r kryptimi). Tokiu atveju žemų dažnių juostoje vidutinio elektrinio lauko stiprio vertės beveik nepriklauso nuo dažnio, tačiau jos padidėja aukštesniųjų dažnių srityje, kai bendraašėje linijoje sužadinama ne tik TEM, bet ir $\rm TE_{11}$ moda. Ribinė normuoto elektrinio lauko stiprio vertė žemų dažnių srityje apytikriai lygi 0,6 ir ji labai artima vertei, apskaičiuotai idealios kliūties atveju (0,64).